Quaternary Science Reviews 29 (2010) 213–221

Contents lists available at ScienceDirect

Quaternary Science Reviews

journal homepage: www.elsevier.com/locate/quascirev

Atmospheric methane isotope records covering the Holocene period

Todd Sowers

The Earth and Environmental Systems Institute, Penn State University, 317B EESB Building, University Park, PA 16802, United States

ARTICLE INFO

Article history:
Received 15 January 2009
Received in revised form
22 May 2009
Accepted 27 May 2009

ABSTRACT

Records of the $^{13}C/^{12}C$ ($\delta^{13}CH_4$) and the D/H (δD_{CH_4}) ratio of atmospheric methane were recovered from the GISP II ice core covering the last 11,000 years. All totaled, 76 samples were analyzed for $\delta^{13}CH_4$ and 65 adjacent samples for δD_{CH_4} between 86 and 1696 m below surface (mbs) providing a temporal resolution that is better than one pair of isotope samples every 200 years. The $\delta^{13}CH_4$ record exhibits a decreasing trend throughout the Holocene beginning at −46.4‰ at 11,000 years BP (BP defined as 1950 AD = 11 ka), and decreasing to −48.4‰ at 1 ka. The 2‰ $\delta^{13}CH_4$ drop is likely to be a combination of increased CH_4 emissions from Arctic lake ecosystems and an increase in the ratio of C_3/C_4 plants in wetlands where CH_4 is emitted. The C_3/C_4 ratio increase is the result of increasing CO_2 values throughout the Holocene combined with the activation of high NH ecosystems that are predominantly C_3 type.

The δD_{CH_4} record over the early-mid Holocene shows a slightly decreasing trend that would be predicted by increased CH_4 emissions from Arctic lakes. Between 4 ka and 1 ka, δD_{CH_4} values increase by ~20‰ while $\delta^{13}CH_4$ values remain effectively constant. There are at least two plausible explanations for this 20‰ δD_{CH_4} shift. First, a dramatic shift in CH_4 emissions from higher latitudes to the tropics could account for the observed shift though the lack of a corresponding $\delta^{13}CH_4$ shift is difficult to reconcile. Secondly, a gradual release of marine clathrates with enriched δD_{CH_4} values explains both the δD_{CH_4} and $\delta^{13}CH_4$ records over this period.

1. Introduction

Atmospheric CH_4 records illustrate variability on numerous timescales. The longest record from the EPICA project covering the last 800,000 years (800 kyr) document low CH_4 values (~350 ppb) during the coldest parts of the glacial periods and relatively high (600–700 ppb) values during warm interglacial periods (Spahni et al., 2005; Loulergue et al., 2008). Embedded within the normal glacial/interglacial cycle, CH_4 variations have a significant amount of variability associated with the 20 kyr precession bandwidth that is attributed to a monsoonal influence on tropical wetland CH_4 emissions (Chappellaz et al., 1990; Brook et al., 1996). Furthermore, millennial scale CH_4 fluctuations appear to be tightly coupled with Dansgaard/Oeschger climate oscillations during glacial periods with higher CH_4 values associated with warmer interstadial periods (Chappellaz et al., 1993). The strong coupling between atmospheric CH_4 values and Greenland temperatures has been interpreted to imply a strong teleconnection between circum-N. Atlantic climate and the global hydrologic cycle (Chappellaz et al., 1993; Brook et al., 1996).

The strong coupling between circum-N. Atlantic climate and CH_4 variations does not, however, hold during the Holocene (Fig. 1). High-resolution CH_4 records covering the Holocene show moderately high CH_4 values (~700 ppb) during the Pre Boreal period (9.5–11 kyr before present, 9.5–11 ka). Between 9.5 and 5.5 ka, CH_4 drops gradually to ~580 ppb before it slowly rises to preindustrial values (~700 ppb) by 1 ka (1000 AD). Finally, the last 200 years show a dramatic CH_4 doubling due to increased anthropogenic emissions making CH_4 the second most important long-lived greenhouse gas in the atmosphere today (Forster et al., 2007). The "bowl" shaped CH_4 curve during the Holocene is disconnected from the stable temperature records that dominate the circum N. Atlantic as illustrated by the isotopic temperature ($\delta^{18}O_{ice}$) record from GISP II in Fig. 1.

Three prominent hypotheses have been put forth to explain the Holocene CH_4 record. The Ruddiman hypothesis posits that early civilizations began to influence atmospheric CH_4 levels beginning about 5 ka (Ruddiman, 2003). The basis for this hypothesis is the strong coupling between CH_4 and NH insolation as modulated by Asian–African monsoons (Loulergue et al., 2008). The hypothesis has been supported by the correlation between decreasing NH insolation and CH_4 concentrations during previous interglacial periods (with the exception of marine isotope stage 11) (Ruddiman

E-mail address: todd.sowers5@gmail.com

0277-3791/$ – see front matter © 2009 Elsevier Ltd. All rights reserved.
doi:10.1016/j.quascirev.2009.05.023

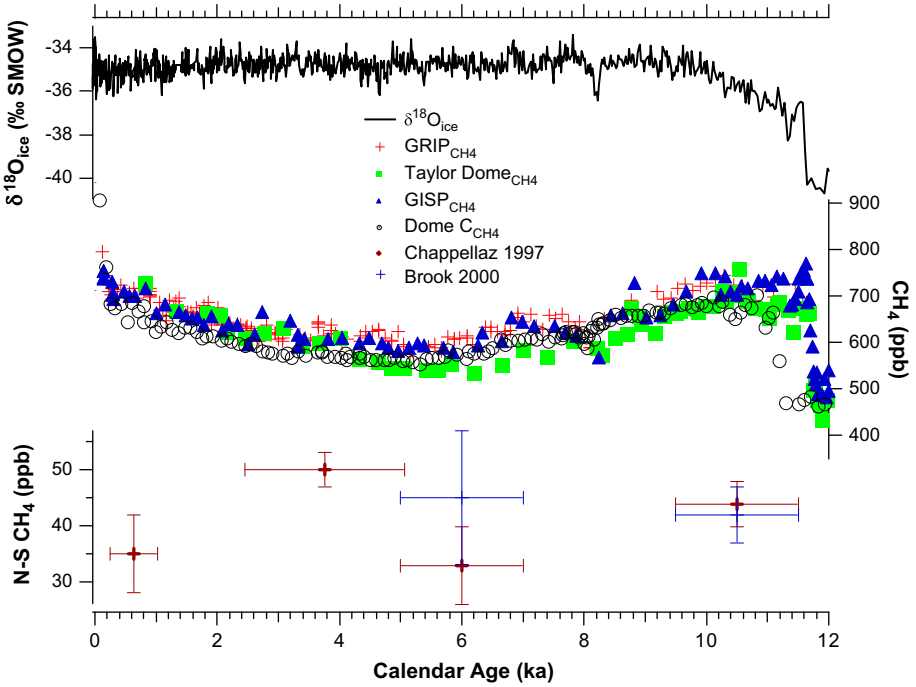

Fig. 1. Methane concentration records covering the Holocene. The upper curve is the isotopic temperature record from GISP II (Grootes et al., 1993). The middle curves are methane concentration records from GRIP (Blunier et al., 1995), Taylor Dome (Brook et al., 2000), GISP II (Brook et al., 1996), Dome C (Flückiger et al., 2002). The bottom portion of the figure illustrates the interpolar CH_4 gradient (IPG) from (Chappellaz et al., 1997), and (Brook et al., 2000).

and Thomson, 2001). Early rice agricultural practices (excessive flooding) yielded higher per capita CH_4 emissions than today such that even though world population was extremely low, humans actually had a progressively higher impact on atmospheric CH_4 loadings between 5 ka and the present. Ruddiman suggests that the decline in the interpolar CH_4 gradient (IPG) between 4 ka and 0.8 ka supports his hypothesis because the population increases during this period were centered on the equator, causing the reduced IPG in the late Holocene.

Another prominent hypothesis put forward to explain the Holocene CH_4 record points to changes in tropical wetland emissions as the primary driving force (Chappellaz et al., 1997). Under this hypothesis, the broad CH_4 minimum at 5 ka is driven by lower tropical CH_4 emissions while, the IPG record is primarily driven by moderate changes in tropical emissions along with more subtle changes in NH wetland emissions. Because tropical wetlands are by far the largest natural source of CH_4 and clearly tied to NH insolation via the monsoons, small changes in the hydrologic cycle in the tropics can yield large changes in atmospheric CH_4 loading over very short time periods.

The third set of ideas put forth to explain the concentration history involves changes in the sink term for atmospheric CH_4. The concentration of CH_4 in the atmosphere is always controlled by the balance between the sources and sinks. Thus, the decreasing concentration trend in the early to mid part of the Holocene could be the result of an increase in the rate at which CH_4 is removed from the atmosphere as opposed to a decrease in the sources. Present day estimates of the primary CH_4 sinks suggest tropospheric OH radicals account for 88% of total while soils and stratospheric destruction make up 5% and 7% of total (Reeburgh, 2004). Tropospheric OH radicals are also the primary sink for volatile organic compounds (VOCs) and CO. As such, changes in the atmospheric loading of these entities will have an impact on the lifetime of atmospheric CH_4 that is independent of the CH_4 sources.

Under steady state conditions, the atmospheric loading and the isotopic composition of tropospheric CH_4 are dictated by the flux-weighted balance of all sources and sinks and their characteristic isotope effects. Atmospheric CH_4 changes can thus be the result of changes in sources, sinks or some combination of the two. CH_4 isotope records from ice cores, therefore, provide fundamental boundary conditions for assessing the cause of observed concentration variations. For example, atmospheric CH_4 levels increased from 450 to 600 ppb near the end of the Younger Dryas period ~11.5 ka. $\delta^{13}CH_4$ and δD_{CH_4} records covering this transition show no discernable trends associated with the increased CH_4 values (Schaefer et al., 2006; Sowers, 2006; Fischer et al., 2008). While there are many plausible explanations for the lack of an isotope signature accompanying this particular concentration increase, the most straightforward explanation maintains a constant proportion of both emissions and sinks, while global sources increase relative to the sink terms. Moreover, the lack of a substantial δD_{CH_4} increase during this period ruled out a massive clathrate destablization event as the cause of the concentration increase (Sowers, 2006).

Important information pertaining to the latitudinal sources of CH_4 can be derived from the interpolar CH_4 gradient (IPG). Because the primary CH_4 sink (tropospheric OH radicals) is uniformly distributed about the equator, the N–S CH_4 IPG is a qualitative measure of N–S source distribution. Continuous atmospheric CH_4 measurements throughout the globe today illustrate the preponderance of NH CH_4 sources that yield IPG estimates for the last two decades between 125 and 145 ppb (Dlugokencky et al., 2003). Historical IPG estimates can be reconstructed from ice cores by analyzing CH_4 in Greenland and Antarctic ice core samples that were occluded at the same time. The accuracy of these paleoIPG estimates depends on how well the two ice core timescales can be established and the analytical uncertainties associated with the CH_4 measurements (Dällenbach et al., 2000). There are two studies that have attempted to reconstruct Holocene IPG values from ice cores. Chappellaz et al. (1997) utilized the D47 and Byrd cores from Antarctica and compared the CH_4 values from these two cores with the GRIP core from Greenland (Fig. 1). Their results showed early

Holocene IPG values of 45 ppb that increased to 50 ppb by 3.7 ka and then dropped to 35 ppb by 0.7 ka. Brook et al. (2000) also measured Holocene IPG using the GISP II and Taylor Dome ice cores with results that were in line with Chappellaz et al. (1997). With the exception of one estimate at 6 ka, the IPG results in Fig. 1 suggest that NH CH_4 emissions decreased less than the tropics between 10.5 and 3.8 ka during which time the total emissions decreased by 14%.

The present contribution focuses on new CH_4 isotope (both $\delta^{13}CH_4$ and δD_{CH_4}) records from the GISP II ice core that cover the Holocene period. After reviewing the relation of the new records to existing records from the start and end of the Holocene, the overall isotope records will be discussed as constraints on the global CH_4 cycle throughout the Holocene. Three time slices will be discussed in detail utilizing a simple two-box model of the atmosphere.

2. Methods

Holocene $\delta^{13}CH_4$ and δD_{CH_4} records were constructed using the GISP II ice core (72° 36′N, 38° 30′W, elevation 3203 m) that was drilled between 1989 and 1993 at the summit of Greenland. We analyzed 76 samples for $\delta^{13}CH_4$ and 65 adjacent samples for δD_{CH_4} between 86 and 1696 m below surface (mbs). The CH_4 isotope data are reported on a gas age vs depth scale developed by Brook et al. (1996) with a temporal resolution that is better than one pair of isotope samples every 200 years.

Trapped gas were liberated from each 0.8–1.6 kg ice sample using a melt/refreeze (wet) extraction technique (Sowers and Jubenville, 2000; Sowers, 2006). Briefly, shaved ice samples were initially placed into an SS vacuum cylinder that was evacuated for 45 min before isolation. The cylinder was then inserted into a warm water bath to melt the ice allowing the occluded air parcels to accumulate in the headspace above the meltwater. The cylinder was then lowered into an SS Dewar with liquid nitrogen to refreeze the water before the cylinder was attached to a helium flow system to flush the headspace. The sample gas stream was initially passed through a water trap (−110 °C) before entering a CH_4 trap made of Haysep D material cooled to −130 °C. The Haysep D CH_4 trap was isolated, removed from the extraction line, and attached to a modified PreCon peripheral device feeding either a MAT 252 ($\delta^{13}CH_4$) or Delta XP^{plus} (δD_{CH_4}) analyzer for standard continuous flow isotope ratio measurements (CF-IRMS). Daily standards were analyzed at the beginning of each analytical day. Results had to fall within 0.3‰ and 3‰ of the assigned $\delta^{13}CH_4$ and δD_{CH_4} values (−47.13‰ VPDB and −84.3‰ VSMOW, respectively) before ice core samples were analyzed. All samples analyzed during a day were corrected for daily standard offsets from the assigned values. Results were reported on the VPDB and SMOW scales for $\delta^{13}CH_4$ and δD_{CH_4}, respectively. All isotope data were corrected for gravitational fractionation using previously published $\delta^{15}N_2$ records (Sowers et al., 1992).

External precision is estimated based on simulated trapped gas extractions that were designed to mimic normal sample extraction protocols as closely as possible. The simulated transfers utilize degassed, bubble free ice (BFI) that was shaved and inserted into an extraction cylinder. After the BFI cylinder was evacuated for 45 min, aliquots of working standard were introduced over the ice. The cylinder was then sealed and the BFI melted and refrozen as per normal protocol. Results of 31 simulated transfers for $\delta^{13}CH_4$ performed before, during and after the GISP II samples were analyzed yielded average $\delta^{13}CH_4$ values that were -0.08 ± 0.3‰ lower than the assigned values suggesting no measurable alteration of the isotopic ratios can be attributed to the extraction procedure. Another 14 simulated transfers were made for δD_{CH_4} yielding an average difference from the assigned value of $+1.3 \pm 3$‰, again suggesting the analytical manipulations did not alter the original isotopic values. We assign the overall uncertainty associated with the $\delta^{13}CH_4$ and δD_{CH_4} measurements based on the BFI simulated transfers as ±0.3‰ and ±3‰ for $\delta^{13}CH_4$ and δD_{CH_4}, respectively.

Samples of firn air from Summit (GISP II) were retrieved in June of 2006. A total of 14 air samples were taken between the surface and the base of the firn/ice transition region (79.6 mbs). $\delta^{13}CH_4$ and δD_{CH_4} results from the upper 10 m of the firn provide an accurate integrated average value for the atmospheric composition over the previous 2–3 years due the diffusive mixing in the porous firn. $\delta^{13}CH_4$ and δD_{CH_4} data between 10 and 79 m provide the means or reconstructing atmospheric $\delta^{13}CH_4$ and δD_{CH_4} records covering the last 50 years. The $\delta^{13}CH_4$ and δD_{CH_4} data were corrected for gravitational fractionation and the diffusive effect of the increasing atmospheric CH_4 on the isotopic composition of CH_4 in the firn following Mischler (2009). The age of the firn air at each level was assessed using the measured CFC-11 values along with an air transport model developed for the site following Battle et al. (1996).

3. Results

All $\delta^{13}CH_4$ and δD_{CH_4} data are plotted in Fig. 2. Each data point is the result of a single ice core analysis with error bars corresponding to the uncertainties deduced from the simulated transfer results. The isotope results are plotted on separate *y* axes that are oriented with "lighter" (more negative) values pointing up on the graph. For reference, present day $\delta^{13}CH_4$ and δD_{CH_4} values are -47.3 ± 0.1‰ and -92.6 ± 2.5‰, respectively based on near surface firn air sampling in 2006.

Over the last two centuries, both $\delta^{13}CH_4$ and δD_{CH_4} have increased from local minima centered around 1750 AD to the present in response to anthropogenic CH_4 emissions that are isotopically enriched relative to preindustrial emissions (Ferretti et al., 2005; Sowers et al., 2005; Mischler, 2009). Between the 18th century and ~1.8 ka, both $\delta^{13}CH_4$ and δD_{CH_4} increased to values that are close to present day. The GISP II $\delta^{13}CH_4$ data show little change from 1 to 4 ka. Before 4 ka, $\delta^{13}CH_4$ data trend almost linearly towards heavier values of −46‰ at 11 ka. Between 1.8 ka and 4 ka, δD_{CH_4} values decrease fairly linearly reaching values around −110‰ at 4 ka. It is important to note that this 20‰ shift occurs during a 3 kyr period when the $\delta^{13}CH_4$ record is effectively stable. The δD_{CH_4} record prior to 4 ka shows relatively stable values (−110‰) but the sample-to-sample variability can be extremely large (~15‰) in some parts of the record. Such variability is unlikely to be related to true atmospheric δD_{CH_4} fluctuations because the large δD_{CH_4} changes occur over short periods of time (~200 years) when both the concentration and $\delta^{13}CH_4$ values remain stable. It is noteworthy that this section of core corresponds to the "brittle ice zone" where increasing hydrostatic pressures cause the air in the bubbles to be enclosed in solid hydrates or clathrates. The quality of the ice core in this section tends to be much worse than ice either above or below with numerous fractures extant in each sample. It is also noteworthy that the $\delta^{13}CH_4$ data from this interval do not show the excessive sample-to-sample scatter that the δD_{CH_4} record shows. While we do not have a clear explanation for these observations, we note that the sample size for the δD_{CH_4} analyses is nearly twice that for the $\delta^{13}CH_4$ analyses. If the δD_{CH_4} anomalies are related to drill fluid infiltration into microfractures then there are more opportunities for contamination impacting the δD_{CH_4} results relative to $\delta^{13}CH_4$ because the samples are twice as long.

4. Data

The new CH_4 isotope records presented in Fig. 2 provide important boundary conditions for assessing the cause of the

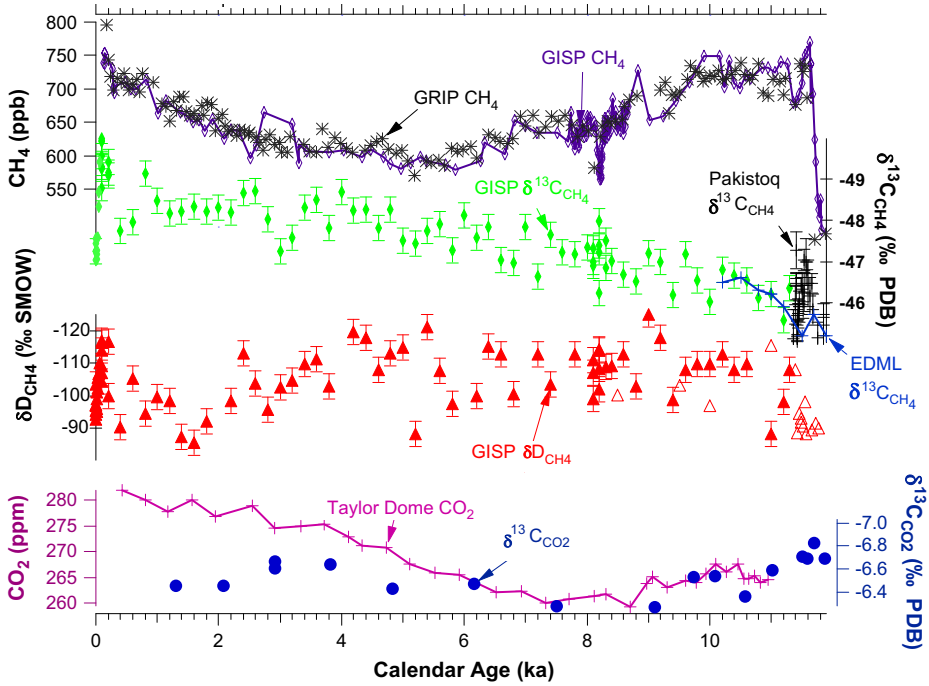

Fig. 2. Trace gas records covering the Holocene. The top two curves are atmospheric CH_4 records from GISP II and GRIP as shown in Fig. 1. The $\delta^{13}CH_4$ and δD_{CH_4} records from GISP II are plotted below the CH_4 records. Note the "inverted" isotope scale (*y*-axes) adopted for plotting purposes. $\delta^{13}CH_4$ records from the early Holocene from Pakistoq (Schaefer et al., 2006) and EDML (Fischer et al., 2008) are included for reference. The bottom data are the CO_2 and $\delta^{13}CO_2$ records from Taylor Dome (Indermühle et al., 1999, 2000).

concentration fluctuations throughout the Holocene. The records can be divided up into three distinct intervals. Moving forward in time, the period between 10.5 and 4 ka show decreasing $\delta^{13}CH_4$ and δD_{CH_4} values though the δD_{CH_4} values exhibit excessive scatter making a trend difficult to establish. Between 4 ka and 1.3 ka, $\delta^{13}CH_4$ values remain effectively stable while δD_{CH_4} increases by ~20‰. Finally, between 1.3 ka and present, both $\delta^{13}CH_4$ and δD_{CH_4} records exhibit a "fish hook" shape with local minima centered in the early part of the 19th century that is presumably related to various anthropogenic activities (Ferretti et al., 2005; Houweling et al., 2008; Mischler, 2009). The isotope records from GISP II over the last 1.3 kyr are not high enough resolution to warrant detailed investigation. It is, however, noteworthy that the shape of the GISP II records over the last 1.3 kyr are very similar to those from Antarctica with offsets resulting from the interpolar isotope gradients. Efforts are currently underway to investigate this interval in greater detail as part of the new NEEM ice core initiative in NE Greenland.

The general trends of the Holocene CH_4 concentration record and either of the isotope records are dissimilar implying there is no single explanation for the observed CH_4 bowl. One plausible explanation for the low CH_4 values during the mid Holocene involves an increase in sink. Were this to be the case, one would expect the isotope records to closely follow the concentration curve and both isotope records would track one another very tightly. It is quite clear from the records that, while we cannot completely rule out changes in the sink term, we can safely say that other factors have driven the isotope records and, by extension, that these factors are likely to have had a major impact on the atmospheric loading.

4.1. Simple box modeling

The primary motivation for this work was to utilize the isotopic records to better constrain the global biogeochemistry of atmospheric CH_4 throughout the Holocene. Studies with similar objectives can generally be divided up into "top-down" or "bottom up" studies. The top-down approach utilizes atmospheric records to infer changes in the CH_4 source/sink terms and use simple models to assess source/sink variations. This approach involves ascribing source/sink changes over large geographic areas which are inherently heterogeneous in space and time. Because the only reliable atmospheric records have been recovered from high latitude Greenland and Antarctic ice cores, there is little historic information that can be learned from tropical regions where the bulk of preanthropogenic wetland CH_4 emissions were located. Moreover, the atmosphere integrates changes in both the sources and sinks such that other studies are needed to sort out the relative contribution of individual sources and sinks to explain the observed concentration changes (Valdes et al., 2005). Those studies that focus on computing global CH_4 sources and sinks within the confines of a GCM are commonly referred to as "bottom up" studies. Here, one has to account for the multitude of biogeochemical parameters that influence the production, transport, and consumption of CH_4 within the biosphere (Valdes et al., 2005; Harder et al., 2007). The ultimate goal of these "bottom up" studies is to target atmospheric reconstructions obtained from the ice cores.

The present contribution is a "top-down" study utilizing new CH_4 isotope records to help explain the CH_4 concentration record. In order to quantify changes in the atmospheric CH_4 budget, a simple two-box model of the troposphere was utilized following Tans (1997). This approach was chosen because we are limited to data from Antarctica and Greenland. Utilizing a model that has more latitudinal resolution or a full blown AGCM is not warranted in this "top-down" approach because we cannot constrain the latitudinal source gradients at this time. The down side of using the two-box model is the difficulty in dealing with the fact that there are substantial interhemispheric gradients that are truncated with only two boxes. Additionally, changes in sources within a hemisphere (e.g. high Arctic emissions) are necessarily lumped together

with low latitudinal emissions so it is impossible to separate the two. Previous studies have addressed latitudinal emission changes using a three box model of atmospheric CH_4 (North, Tropical, and Southern boxes) to separate the tropical emissions from the high latitude emissions (Chappellaz et al., 1997; Brook et al., 2000). This approach was not selected for the present study due to a lack of information for constraining tropical emissions relative to the high latitude sources.

Each of the two boxes in the Tans model corresponds to the two tropospheric hemispheres. The lifetime of CH_4 in both boxes and the exchange between the two boxes across the equator are fixed at 7.6 years and 0.9 years, respectively (Lelieveld et al., 1998; Houweling et al., 2000). The characteristic isotope fractionation factors ascribed to the sink process were a weighted mean of present day estimates for the three sink terms (OH, soils, and stratospheric uptake) (Mischler et al., submitted for publication). The flux-weighted fractionation factors were held constant at 0.9946 and 0.7731 for $^{13}C/^{12}C_{CH4}$ and D/H_{CH_4}, respectively. The inputs to the model are the emissions and mean isotopic composition of CH_4 added to each hemispheric box. Each simulation is run for 150 years with the simulations reaching steady state after the first 50 years.

The model was applied at three periods corresponding to the boundaries between the three intervals deduced from the CH_4 isotope records mentioned earlier (1 ka, 4 ka, and 10.5 ka). It is fortuitous that these breaks in the isotope records occur almost exactly where Chappellaz et al. (1997) made discrete IPG estimates such that we can use the IPG estimates as constraints in the model simulations. As mentioned, one shortcoming of using the two box model approach is the poor treatment of the true latitudinal gradients. To correct for the model shortcoming, we follow Etheridge et al. (1998) and assign the global mean values (both concentration and isotopic values) as the Antarctic values plus 37% of the N–S gradient. In the two-box model, the difference between the two hemispheric model boxes would be 74% of the observed N–S gradient observed between Greenland and Antarctica. Because we have NH data (GISP II), we set the NH model box target values to the measured value from GISP II minus 26% of the interhemispheric gradient.

As we do not have Holocene $\delta^{13}CH_4$ and δD_{CH_4} records from Antarctica to compliment our GISP II data and constrain the model, a control run was constructed using the N–S CH_4 gradient, $\delta^{13}CH_4$ and δD_{CH_4} data from GISP II and the lower section of a short core from WAIS Divide WDC05A covering the preindustrial period between 990 AD and 1400 AD (Mischler, 2009). These results were generated using the same extraction procedure and standards as the GISP II data providing a solid basis for comparison. Between 990 and 1400 AD, the Antarctic WDC05A isotope results are enriched in the heavy isotopes relative to the GISP II data yielding interhemispheric (N–S) $\delta^{13}CH_4$ and δD_{CH_4} gradients of $-1.0 \pm 0.4‰$ and $-12 \pm 6‰$, respectively. For comparison, surface values obtained during firn air experiments at both GISP II and WAIS yield present day $\delta^{13}CH_4$ and δD_{CH_4} gradients of $-0.3 \pm 0.1‰$ and $-13 \pm 3‰$, respectively.

All target data that was used to determine the flux and mean isotopic composition of CH_4 added to the two boxes for the 1 ka control run is tabulated in Table 1. The input emission and isotopic values were then varied until the model results matched the observed data at 1 ka. The resulting CH_4 emissions are 157 and 88 Tg/yr for the Northern and Southern Hemisphere (SH) boxes, respectively. The mean $\delta^{13}CH_4$ of CH_4 added to the two boxes was $-53.0‰$ and $-46.0‰$ for N and S, respectively while the corresponding δD_{CH_4} values were $-296‰$ and $-235‰$ (Table 2). These results are in good agreement with tabulated mean input values for the preindustrial Holocene from Whiticar and Schaefer (2007). Non-exhaustive sensitivity runs were made to establish the uncertainty associated with each of the six input variables (N and S emissions, $\delta^{13}CH_4$ and δD_{CH_4}) given the uncertainties associated with the 1 ka ice core observations in Table 1. These runs suggest the emissions can be constrained to ± 5 Tg/yr, the characteristic $\delta^{13}CH_4$ values to $\pm 0.5‰$, and the δD_{CH_4} values to $\pm 5‰$. It is noteworthy that the resulting $\delta^{13}CH_4$ and δD_{CH_4} source values for the SH are higher than the NH by 7‰ and 61‰, respectively. The primary factor driving the difference between the two hemispheric source values is the interpolar gradients and the characteristic exchange time for air between the two hemispheres (0.9 years). In particular, the large N–S $\delta^{13}CH_4$ difference at 1 ka ($-1.0 \pm 0.4‰$) requires an SH source value of $-46.0‰$.

4.2. Investigating the Holocene CH_4 budget

Assessing the biogeochemistry of CH_4 before 1 ka is more complicated due to the lack of SH CH_4 isotope records. To extend our investigation back in time we therefore need to impose some additional constraints on the box modeling. Given the lack of information from the SH and the lower overall contribution ($\sim 35\%$) to the global CH_4 budget, we have fixed the $\delta^{13}CH_4$ and δD_{CH_4} values for the SH CH_4 emissions with the values obtained from the 1 ka control run ($-46‰$ and $-235‰$, respectively). The NH concentration data and the IPG data from Chappellaz et al. (1997) were then used to constrain the emissions in both hemispheres. The mean $\delta^{13}CH_4$ and δD_{CH_4} values for NH emissions were varied until the model output matched the NH GISP II measurements (Table 1).

There are two primary results from this modeling exercise. First, between 10.5 and 4 ka the $\delta^{13}C$ of NH CH_4 emissions decreased by 1.9‰ while the δD values remained effectively constant. Second, between 4 ka and 1 ka, the $\delta^{13}C$ of NH emissions remained constant while δD values increased by 18‰. These new isotope results provide new information for investigating the Holocene budget.

5. Discussion

Northern hemisphere climate during the early Holocene was supported by elevated NH summer insolation and increased seasonality (Berger and Loutre, 2004) leading to enhanced Asian monsoons and a general northward migration of the ITCZ (Haug et al., 2001; Wang et al., 2005). These conditions were optimum for early wetland development with consequent high CH_4 emissions from the NH wetlands (MacDonald et al., 2006). After the 9 ka NH insolation maximum, declining seasonality reduced the intensity of the monsoon (Wanner et al., 2008) with a concomitant decrease in wetland implying a decrease in wetland emissions contributing to the decline in atmospheric loading over the first half of the Holocene (Fig. 1). While it is difficult to characterize large scale changes in landforms in response to climate changes, Wanner et al. (2008) arrive at the following conclusions that specifically apply to the later half of the Holocene but generally apply to the entire Holocene: "(1) desertification in the African and southwest Asian subtropics related to the weakening of the Afro-Asian monsoon system, (2) shifts in NH temperate forest types and modest southward migration of the Arctic treeline related to the gradual reduction in NH summertime solar forcing, and (3) anthropogenic deforestation and draining of wetlands to create cropland and pasture, concentrated mainly in eastern and southern Asia, the Mediterranean, and Europe." In general, all three of these observations would signal decreased CH_4 emissions with the emphasis being placed on the NH. The increase in the interpolar gradient from 44 to 50 ppb between 10.5 and 4 ka suggests an increase in the relative NH emissions during that period (Chappellaz et al., 1997; Brook et al., 2000). This suggests that while emissions were declining in both hemispheres in concert with NH insolation, SH

Table 1
Holocene time-slice observations.

Time slice (ka)	NH [CH_4] (ppb)[a]	IPG (ppb)[a]	NH $\delta^{13}CH_4$ (‰ PDB)[b]	SH $\delta^{13}CH_4$ (‰ PDB)[c]	NH δD_{CH_4} (‰ SMOW)[b]	SH δD_{CH_4} (‰ SMOW)[c]
1 (N)	710 ± 2 (31)	35 ± 7	−48.4 ± 0.4 (7)	−47.4 ± 0.2 (22)	−95 ± 7 (7)	−83 ± 3 (9)
4 (N)	617 ± 2 (29)	50 ± 3	−48.3 ± 0.3 (6)	N/A	−113 ± 6 (6)	N/A
10.5 (N)	718 ± 2 (18)	44 ± 4	−46.4 ± 0.3 (6)	N/A	−110 ± 9 (6)	N/A

[a] Number of measurements considered are in parentheses (Chappellaz et al., 1997).
[b] Isotope values were averaged over a 1200 year period centered on the time slice. Number of measurements considered are in parentheses.
[c] Isotope values from WAIS Divide core WDC05A with gas ages between 990 and 1405 AD (Mischler, 2009).

emissions declined slightly more than the NH emissions presumably in response to a less vigorous SH hydrologic cycle. Between 4 and 1 ka, the interhemispheric gradient declined suggesting a disproportionate increase of SH emissions during the rise in global loading.

5.1. The CH_4 story between 4 and 10.5 ka

Our two-box model results suggest that the mean $\delta^{13}C$ of NH CH_4 emissions decreased by 1.9‰ between 10.5 ka and 4 ka. Additionally, the δD_{CH_4} values remained effectively constant or decreased slightly over this period. There are at least three plausible explanations for this observation; 1) a progressive increase in CH_4 emissions from Arctic lakes and wetlands, 2) a gradual increase in the ratio of C_3/C_4 plants in areas where CH_4 is emitted, or 3) an increase in methanogenic communities utilizing the CO_2 reduction pathway as compared to the acetate fermentation pathway. In all likelihood, the true explanation for the observed records in Fig. 2 probably involved all three factors in varying degrees throughout the early-mid Holocene.

Present day estimates of CH_4 emissions from thermokarst lakes in the Arctic region are ~20 ± 7 Tg/yr (Walter et al., 2007). These high Arctic emissions are thought to have contributed substantially to the deglacial CH_4 increase as these areas warmed during the termination. While there are fewer ^{14}C dated lakes within the Holocene compared to the termination itself, lakes do appear to be increasingly active CH_4 emitters throughout the Holocene (Walter et al., 2007). Isotope measurements of CH_4 emissions from these lake systems show extremely depleted values ($\delta^{13}CH_4$ and δD_{CH_4} values of −70‰ and −390‰, respectively) (Walter et al., 2008). If one assumes that 19.6 Tg/yr of new CH_4 were gradually added to the NH source term from these lake systems throughout the Holocene, then the $\delta^{13}CH_4$ and δD_{CH_4} of the atmosphere would have dropped by 2.0‰ and 10‰, respectively. A postulated increase in thermokarst CH_4 emissions would require a decline in other areas in order to maintain the total global emissions at ~240 Tg/yr. This estimate is roughly consistent with the observed isotopic trends between 10.5 and 4 ka (1.9‰ and 3‰; Fig. 2, Table 1), though the δD_{CH_4} predicted shift is somewhat larger than the poorly constrained δD_{CH_4} record.

Circumarctic wet and peat lands currently contribute between 20 and 45 Tg of CH_4 to the atmosphere each year (Mikaloff Fletcher et al., 2004). The areal extent of these ecosystems has expanded throughout the Holocene as the ice sheets melted and the ice-covered environments respond to the ice free climatic conditions. The quantity and isotopic composition of CH_4 emitted from these ecosystems today varies considerably depending on the water table, plant type, NEP, and the consortia of methanogens within the ecosystems (Bellisario et al., 1999; Popp et al., 1999; Chanton et al., 2006). Those methanogens that utilize the CO_2 reduction pathway tend to produce CH_4 that is ~35‰ more depleted in the heavy carbon isotope relative to acetoclastic methanogens in the same environment (Valentine et al., 2004, Table 5). Therefore, one way to explain the 1.9‰ $\delta^{13}CH_4$ drop between 10.5 and 4 ka would be to decrease the fraction of CH_4 emitted to the atmosphere by acetoclastic methanogenisis by 5% relative to those methanogens utilizing the CO_2 reduction pathway. This scenario is also consistent with the δD_{CH_4} record if the shift to CO_2 reduction occurred without substantial changes in the geographic distribution of CH_4 emissions.

Another way to explain the isotope variations observed during the first part of the Holocene is by invoking large changes in the ratio of C_3 to C_4 type plants that provide the substrate carbon for terrestrial methanogenisis. C_3 plants utilize the standard Calvin Cycle where a ribulose bisphosphate carboxylase (Rubisco) enzyme fixes CO_2 yielding 3-phosphoglycerate (PGA). In C_3 plants CO_2 must diffuse from the atmosphere/stomata across the mesophyll sheath cells for fixation. C_4 plants, on the other hand, fix CO_2 in the outer mesophyll cells using the PEP carboxylase enzyme (4 carbon molecule) which is then actively shuttled to the inner bundle sheath cells where CO_2 is liberated for subsequent fixation via the standard Calvin Cycle. In relatively humid environments, the passive transport system in C_3 plants (lower energy required per unit CO_2 fixed) allows C_3 plants to outcompete C_4 plants when atmospheric CO_2 levels are high (Ehleringer et al., 1997). High-light and low humidity and CO_2 conditions, however, tend to favor C_4 plants due to their lower evapotranspiration rates. Present day estimates suggest that C_4 plants account for 18–23% of total gross primary production on land today (Ehleringer et al., 1997; Still et al., 2003). However, during the last glacial maximum when atmospheric CO_2 levels were ~190 ppm, C_4 plants were much more pervasive (Collatz et al., 1998).

Isotope discrimination during the transfer of CO_2 into plants causes the characteristic $\delta^{13}C$ value of C_3 and C_4 plants to be ~−25‰ and −16‰, respectively (Farquhar et al., 1989). While there are numerous factors that influence the $\delta^{13}C$ of CH_4 emitted from a particular landscape, changes in the $\delta^{13}C$ of the substrate carbon utilized by methanogens should translate roughly 1:1 into changes in $\delta^{13}CH_4$ if all other factors are held constant. As atmospheric CO_2 is the ultimate source of carbon for methanogenic communities, it stands to reason that changes in $\delta^{13}CO_2$ would have directly influenced $\delta^{13}CH_4$. Analyses of the $\delta^{13}C$ of atmospheric CO_2 throughout the Holocene from the Taylor Dome ice core show little variation (−6.5 ± 0.13‰ PDB (Indermühle et al., 1999), Fig. 2) implying other factors must be responsible for the $\delta^{13}CH_4$ change.

Table 2
Two-box model emission results that satisfy the time-slice observations.

Time (ka)	NH F_{CH_4} (Tg/yr)	SH F_{CH_4} (Tg/yr)	NH $\delta^{13}CH_4$ (‰ PDB)	SH $\delta^{13}CH_4$ (‰ PDB)	NH δD_{CH_4} (‰ SMOW)	SH δD_{CH_4} (‰ SMOW)
1	157 ± 5	88 ± 4	−53.0 ± 0.4	−46 ± 0.5	−296 ± 5	−235 ± 7
4	154	55	−53.0	−46	−308	−235
10.5	166	79	−51.3	−46	−307	−235

In order to account for the full 1.9‰ $\delta^{13}CH_4$ decrease between 10.5 and 4 ka, one would need the percentage of C_4 plants in the early Holocene to account for ~40% of the gross primary production in wetlands which then decreased to present day values of ~20% (Still et al., 2003). There are two independent observations that qualitatively support this contention. First, atmospheric CO_2 levels in the early Holocene were ~265 ppm and increased gradually throughout the Holocene. Low CO_2 levels in the early Holocene favored C_4 plants relative to the late Holocene thereby contributing to the decreasing $\delta^{13}CH_4$. However, due to the plethora of other factors influencing the C_3/C_4 ratio it is difficult to quantify the predicted ratio change that is directly related to the CO_2 changes. It is noteworthy in this context that the large $\delta^{13}CH_4$ change measured throughout the last glacial termination (Fischer et al., 2008), is consistent with a large C_3/C_4 ratio increase that was driven by the large atmospheric CO_2 change (80 ppm) (Collatz et al., 1998). The second factor contributing to an increase in the global C_3/C_4 ratio during the Holocene was newly exposed land areas north of 40°N associated with ice retreat. Today these areas are dominated by C_3 plants (Still et al., 2003) which were presumably inactive during the last glacial period due to ice cover. As the ice margin retreated northward during the deglaciation, warmer temperatures would have thawed these areas thereby activating their methanogenic communities. The CH_4 from this region with characteristic low $\delta^{13}CH_4$ values would have contributed to the decreasing atmospheric $\delta^{13}CH_4$ in the early to mid Holocene.

5.2. The CH_4 story between 1 and 4 ka

The isotopic composition of atmospheric methane between 1 and 4 ka is intriguing. The $\delta^{13}C$ of CH_4 is nearly constant throughout this period while δD_{CH_4} values increase by nearly 20‰ between 4 ka and 1 ka. The magnitude of this increase rivals that associated with the δD_{CH_4} change associated with the last glacial termination (Sowers, 2006). This late Holocene δD_{CH_4} signal not only has almost no corresponding $\delta^{13}C$ change, but it also occurs during a period of modest concentration increase (~90 ppb) and a substantial lowering of the IPG suggesting an SH/tropical source.

The D/H ratio of terrestrial CH_4 has been shown to follow the δD of local water (Waldron et al., 1999; Chanton et al., 2006). In general, the δD of meteoric water decreases with distance from the source through Raleigh type distillation (Jouzel et al., 2000). The most straightforward explanation for the dramatic δD_{CH_4} increase between 4 and 1 ka involves a shift towards tropical CH_4 emissions. Based on the rather limited data available for wetlands, δD_{CH_4} values range from −300‰ in tropical wetlands to −400‰ in extremely high latitudes (Waldron et al., 1999; Chanton et al., 2006). If one were to assume the tropics and high latitude wetlands had end member δD_{CH_4} values of −300‰ and −400‰ respectively, then the 20‰ δD_{CH_4} increase between 4 and 1 ka would require a 20% shift in CH_4 emissions from high latitude to tropical areas which is roughly consistent with the decreased IPG over this same period. Under this scenario, the increased tropical emissions would need to have the same $\delta^{13}CH_4$ as that from the higher latitudes. Unfortunately, there are very few paired $\delta^{13}CH_4$ and δD_{CH_4} wetland studies to assess this possibility.

One other potential explanation for the 20‰ δD_{CH_4} increase between 4 and 1 ka involves a gradual release of marine clathrates which have characteristic $\delta^{13}CH_4$ and δD_{CH_4} values of −60‰ and −186‰, respectively (Milkov, 2005). The clathrate $\delta^{13}CH_4$ values are very similar to the average NH value (−53.5‰) so increased clathrate emissions will not have influenced the atmospheric $\delta^{13}CH_4$ (Schaefer et al., 2006). On the other hand, clathrate δD_{CH_4} values are considerably higher than the δD_{CH_4} values for either hemisphere (Table 2) such that destabilizing marine clathrates would drive atmospheric δD_{CH_4} values higher in accordance with our observations between 4 and 1 ka. All totaled, an additional 20 Tg/yr (=9.5% of total) of clathrate CH_4 would be needed to account for the 20‰ δD_{CH_4} increase. This value is the extreme case given some portion of the marine based clathrates would be consumed within the water column (Whiticar and Faber, 1986) causing the fraction of clathrate CH_4 crossing the air/sea interface to be even more enriched. The question one might then ask in this respect is whether there is any evidence for clathrate destabilization over this period in marine sedimentary sequences? In the Santa Barbara basin, where foraminiferal $\delta^{13}C$ evidence has been used to suggest clathrate destabilization episodes during the last glacial period (Kennett et al., 2000) there is no clathrate $\delta^{13}C$ signature to support a late Holocene destablization event. Moreover, the inferred clathrate CH_4 would need to have been slowly added to the atmosphere between 4 and 1 ka to account for the gradual δD_{CH_4} increase. The gradual clathrate carbon addition (as CH_4) to the global oceanic carbon pool would be difficult to detect in marine sedimentary $\delta^{13}C$ sequences because the added clathrate carbon is such a small fraction of either the oceanic carbon pool or that oceanic carbon that is fixed each year (Houghton, 2007).

The Ruddiman hypothesis posits that the increased CH_4 levels between 4 and 1 ka are the result of anthropogenic activities that are centered on agriculture. Do the $\delta^{13}CH_4$ and δD_{CH_4} records covering this period provide any support for this hypothesis? The short answer to this question is no, the isotope data do not bear on the Ruddiman hypothesis because we cannot predict the characteristic isotope signature associated with the hypothesized agricultural emissions. However, if we use the present day isotope values for rice and ruminants (Quay et al., 1999) as applicable to the new agricultural emissions between 4 and 1 ka, then we can say with confidence that the $\delta^{13}CH_4$ and δD_{CH_4} records do not support Ruddiman because these inferred isotope values are lower than the flux-weighted global emission values at 4 ka (Table 2). Under the Ruddiman scenario using present day isotope signatures, one would expect both $\delta^{13}CH_4$ and δD_{CH_4} values to decrease between 4 and 1 ka. The 20‰ atmospheric δD_{CH_4} increase over this period is opposite in sign to that expected and the $\delta^{13}CH_4$ data show no discernable trend. It must be emphasized that this inference is highly speculative. Trying to assess the characteristic isotope signatures associated with early civilization methane emissions is a task that is beyond the scope of the current study.

6. Conclusions

The isotopic records of atmospheric methane covering the Holocene provide fundamental boundary constraints for assessing the cause of the concentration changes. The "bowl" shaped concentration history is disconnected from both isotope records suggesting multiple factors are needed to explain both the concentration and isotope records. $\delta^{13}CH_4$ values measured on the GISP II ice core covering the early Holocene were in good agreement with previous measurements which are ~2‰ higher than present day (and preanthropogenic) values. The $\delta^{13}CH_4$ record exhibits a near linear decrease throughout the Holocene in response to a combination of two factors. First, the Arctic lake ecosystems have recently been shown to emit substantial amounts of CH_4 (Walter et al., 2007, 2008). If these lake emissions have increased by ~19.6 Tg/yr during the Holocene, then their low $\delta^{13}CH_4$ values would have contributed to the 1.9‰ reduction in atmospheric $\delta^{13}CH_4$. Another plausible factor contributing to the gradual $\delta^{13}CH_4$ decrease is an increase in the C_3/C_4 ratio in wetlands where methane is emitted. Increased C_3/C_4 ratios would result from increasing atmospheric CO_2 levels as well as the activation of large landmasses in the high NH that are dominated by C_3 plants today.

Quantification of the global C_3/C_4 change during the Holocene is complicated by the numerous other factors that influence this ratio.

The D/H ratio of atmospheric methane shows a slight downward trend during the first half of the Holocene. Because δD_{CH_4} values are strongly modulated by the δD of meteoric water which decreases with latitude, one would expect a covariation between $\delta^{13}CH_4$ and δD_{CH_4} (as observed between 10.5 and 4 ka) if NH CH_4 emissions increased. Between 4 ka and 1 ka, δD_{CH_4} increased by 20‰ while $\delta^{13}CH_4$ values remained effectively constant. The best explanation for this observation is a gradual release of clathrate CH_4 because clathrate $\delta^{13}CH_4$ values are fairly close to the flux-weighted global $\delta^{13}CH_4$ values while the δD_{CH_4} values are much higher (−180‰) compared with the global average (−300‰).

Acknowledgments

Support for this research was provided by a NSF grants OPP-0520470, 0440759 and 0538538. Core curation and sample allocation were handled by the outstanding staff at the National Ice Core Laboratory (NICL). Additional technical help in the lab was afforded by Denny Walizer and George Wood.

References

Battle, M., Bender, M., Sowers, T., Tans, P., Butler, J., Elkins, J., Conway, T., Zhang, N., Lang, P., Clarke, A.D., 1996. Histories of atmospheric gases from the firn at South Pole. Nature 383, 231–235.

Bellisario, L.M., Bubier, J.L., Moore, T.R., Chanton, J.P., 1999. Controls on CH_4 emissions from a northern peatland. Global Biogeochemical Cycles 13, 81–91.

Berger, A., Loutre, M.F., 2004. Astronomical theory of palaeoclimates. Comptes Rendus Geoscience 336, 701–709.

Blunier, T., Chappellaz, J., Schwander, J., Stauffer, B., Raynaud, D., 1995. Variations in atmospheric methane concentration during the Holocene epoch. Nature 374, 46–49.

Brook, E., Sowers, T., Orchardo, J., 1996. Rapid variations in atmospheric methane concentration during the past 110,000 years. Science 273, 1087–1091.

Brook, E.J., Harder, S., Severinghaus, J., Steig, E., Sucher, C., 2000. On the origin and timing of rapid changes in atmospheric methane during the last glacial period. Global Biogeochemical Cycles 14, 559–572.

Chanton, J.P., Fields, D., Hines, M.E., 2006. Controls on the hydrogen isotopic composition of biogenic methane from high-latitude terestrial wetlands. Journal of Geophysical Research 111.

Chappellaz, J., Barnola, J.-M., Raynaud, D., Korotkevich, Y.S., Lorius, C., 1990. Atmospheric CH_4 record over the last climatic cycle revealed by the Vostok ice core. Nature 345, 127–131.

Chappellaz, J., Blunier, T., Kints, S., Dallenbach, A., Barnola, J.-M., Schwander, J., Raynaud, D., Stauffer, B., 1997. Changes in the atmospheric CH_4 gradient between Greenland and Antarctica during the Holocene. Journal of Geophysical Research 102, 15,987–15,998.

Chappellaz, J., Blunier, T., Raynaud, D., Barnola, J.M., Schwander, J., Stauffer, B., 1993. Synchronous changes in atmospheric CH_4 and Greenland climate between 40 and 8 kyr BP. Nature 366, 443–445.

Collatz, G.J., Berry, J.A., Clark, J.S., 1998. Effects of climate and atmospheric CO_2 partial pressure on the global distribution of C_4 grasses: present, past and future. Oecologia 114, 441–454.

Dällenbach, A., Blunier, T., Flückiger, J., Stauffer, S., Chappellaz, J., Raynaud, D., 2000. Changes in the atmospheric CH_4 gradient between Greenland and Antarctica during the last glacial and the transition to the Holocene. Geophysical Research Letters 27, 1005–1008.

Dlugokencky, E.J., Houweling, S., Bruhwiler, L., Masarie, K.A., Lang, P.M., MIller, J.B., Tans, P., 2003. Atmospheric methane levels off: temporary pause or new steady-state? Geophysical Research Letters 30. doi:10.1029/2003GL018126.

Ehleringer, J.R., Cerling, T.E., Helliker, B.R., 1997. C_4 photosynthesis, atmospheric CO_2, and climate. Oecologia 112, 285–299.

Etheridge, D.M., Steele, L.P., Francey, R.J., Langenfields, R.L., 1998. Atmospheric methane between 1000 A.D. and present: evidence of anthropogenic emissions and climatic variability. Journal of Geophysical Research 103, 15,979–15,993.

Farquhar, G.D., Ehleringer, J.R., Hubick, K.T., 1989. Carbon isotope descrimination and photosynthesis. Annual Review of Plant Physiology and Plant Molecular Biology 40, 503–537.

Ferretti, D., MIller, J.B., White, J.W.C., Etheridge, D.M., Lassey, K.R., Lowe, D., MacFarling, C., Dreier, M., Trudinger, C., van Ommen, T., Langenfelds, R.L., 2005. Unexpected changes to the global methane budget over the past 2000 years. Science 309, 1714–1717.

Fischer, H., Behrens, M., Bock, M., Richter, U., Schmitt, J., Loulergue, L., Chappellaz, J., Spahni, R., Blunier, T., Leuenberger, M., Stocker, T., 2008. Changing boreal methane sources and constant biomass burning during the last termination. Nature 452.

Flückiger, J., Monnin, E., Stauffer, B., Schwander, J., Stocker, T., Chappellaz, J., Raynaud, D., Barnola, J.-M., 2002. High-resolution Holocene N_2O ice core record and its relationship with CH_4 and CO_2. Global Biogeochemical Cycles 16. doi: 10.1029/2001GB001417.

Forster, P., Ramaswamy, V., Artaxo, P., Berntsen, t., Betts, R., Fahey, D.W., Haywook, J., Lean, J., Lowe, D., Myhre, G., Nganga, J., Prinn, R., Raga, G., Schulz, M., Dorland, R.V., 2007. Changes in atmospheric constituents and in radiative forcing. In: Solomon, S., Qin, D., Manning, M., Chen, Z., Marquis, M., Averyt, K.B., Tignor, M., Miller, H.L. (Eds.), Climate Chagte 2007: the Physical Science Basis. Contribution of Working Group I to the Fourth Assessment Report of the Intergovernmental Panel on Climate Change. Cambridge University Press, Cambridge, UK and New York, NY (Chapter 2).

Grootes, P.M., Stuiver, M., White, J.W.C., Johnsen, S., Jouzel, J., 1993. Comparison of oxygen isotope records from the GISP2 and GRIP Greenland ice cores. Nature 366, 552–554.

Harder, S.L., Shindell, D.T., Schmidt, G.A., Brook, E.J., 2007. A global climate model study of CH_4 emissions during the Holocene and glacial–interglacial transitions constrained by ice core data. Global Biogeochemical Cycles 21.

Haug, G., Hughen, K., Sigman, D., Peterson, L., Rohl, U., 2001. Southward migration of the intertropical convergence zone through the Holocene. Science 293, 1304.

Houghton, R.A., 2007. Balancing the global carbon budget. Annual Reviews of Earth and Planetary Sciences 35, 313–347.

Houweling, S., Dentener, G., Lelieveld, J., 2000. Simulation of preindustrial atmospheric methane to constrain the global source strength of natural wetlands. Journal of Geophysical Research 105, 17,243–17,255.

Houweling, S., Van der Werf, G.R., Goldewijk, K.K., Rockmann, T., Aben, I., 2008. Early anthropogenic CH_4 emissions and the variation of CH_4 and $23CH_4$ over the last millennium. Global Biogeochemical Cycles 22.

Indermühle, A., Monnin, E., Stauffer, B., Stocker, T., Wahlen, M., 2000. Atmospheric CO_2 concentration from 0 to 20 KyrBP from the Taylor Dome ice core, Antarctica. Geophysical Research Letters 27, 735–738.

Indermühle, A., Stocker, T.F., Fischer, H., Smith, H.J.F.J., Wahlen, M., Deck, B., Mastroianni, D., Tschumi, J., Blunier, T., Meyer, R., Stauffer, B., 1999. Holocene carbon-cycle dynamics based on CO_2 trapped in ice at Taylor Dome, Antarctica. Nature 398, 121–126.

Jouzel, J., Hoffmann, G., Koster, R.D., Masson, V., 2000. Water isotopes in precipitation: data/model comparison for present-day and past climates. Quaternary Science Reviews 19, 363–379.

Kennett, J.P., Cannariato, K.G., Hendy, I.L., Behl, R.J., 2000. Carbon isotopic evidence for methane hydrate instability during Quaternary interstadials. Science 288, 128–133.

Lelieveld, J., Crutzen, P.J., Dentener, F.J., 1998. Changing concentration, lifetime and climate forcing of atmospheric methane. Tellus 58, 128–150.

Loulergue, L., Schilt, A., Spahni, R., Masson-Delmotte, V., Blunier, T., Lemieux, B., Barnola, J.-M., Raynaud, D., Stocker, T., Chappellaz, J., 2008. Orbital and millennial-scale features of atmospheric CH_4 over the past 800,000 years. Nature 453, 383–386.

MacDonald, G.M., Beilman, D.W., Kremenetski, K.V., Sheng, Y., Smith, L.C., Velichko, A.A., 2006. Rapid early development of circumarctic peatlands and atmospheric CH_4 and CO_2 variations. Science 314, 285–288.

Mikaloff Fletcher, S.E., Brunhwiler, L.M., MIller, J.B., Heimann, M., 2004. CH_4 sources estimated from atmospheric observations of CH_4 and its 13C/12C isotopic ratios: inverse modeling of sources processes. Global Biogeochemical Cycles 18. doi:10.1029/2004GB002223.

Milkov, A.V., 2005. Molecular and stable isotope composition of natural gas hydrates: a revised global dataset and basic interpretations in the context of geological settings. Organic Geochemistry 36, 681–702.

Mischler, J.M., 2009. Carbon and hydrogen isotopic composition of methane over the last 1000 years. Unpublished Masters thesis, Pennsylvania State University.

Mischler, J.M., Sowers, T.A., Alley, R.B., Battle, M., McConnell, J., Mitchell, L., Popp, T., Sofen, E., Spencer, M. Carbon and hydrogen isotopic composition of methane over the last 1000 years. Global Biogeochemical Cycles, submitted for publication.

Popp, T.J., Chanton, J.P., Whiting, G.J., Grant, N., 1999. Methane stable isotope distribution at a Carex dominated fen in North central Alberta. Global Biogeochemical Cycles 13, 1063–1077.

Quay, P., Stutsman, J., Wilbur, D., Snover, A., Dlugokencky, E., Brown, T., 1999. The isotopic composition of atmospheric methane. Global Biogeochemical Cycles 13, 445–461.

Reeburgh, W.S., 2004. Global methane biogeochemistry. In: Keeling, R.F. (Ed.), The Atmosphere. Treatise on Geochemistry. Elsevier-Pergamon, Oxford, pp. 65–90.

Ruddiman, W.F., 2003. The anthropogenic greenhouse era began thousands of years ago. Climatic Change 61, 261–293.

Ruddiman, W.F., Thomson, J.S., 2001. The case for human causes of increased atmospheric CH_4 over the last 5000 years. Quaternary Science Reviews 20, 1769.

Schaefer, H., Whiticar, M.J., Brook, E., Petrenko, V.V., Ferretti, D., Severinghaus, J., 2006. Ice record of d13C for atmospheric CH_4 across the Younger Dryas-Preboreal transition. Science 313, 1109–1112.

Sowers, T., 2006. Late Quaternary atmospheric CH_4 isotope record suggests marine clathrates are stable. Science 311, 838–841.

Sowers, T., Bender, M., Raynaud, D., Korotkevich, Y.S., 1992. The $\delta^{15}N$ of N_2 in air trapped in polar ice: a tracer of gas transport in the firn and a possible constraint on ice age-gas age differences. Journal of Geophysical Research 97, 15,683–15,697.

Sowers, T., Bernard, S., Aballain, O., Chappellaz, J., Barnola, J.-M., Marik, T., 2005. Records of the d13C of atmospheric CH4 over the last two centuries as recorded in Antarctic snow and ice. Global Biogeochemical Cycles 19.

Sowers, T., Jubenville, J., 2000. A modified extraction technique for liberating occluded gases from ice cores. Journal of Geophysical Research 105, 29,155–29,164.
Spahni, R., Chappellaz, J., Stocker, T., Loulergue, L., Hausammann, G., Kawamura, K., Fluckiger, J., Schwander, J., Raynaud, D., Masson-Delmotte, V., Jouzel, J., 2005. Atmospheric methane and nitrous oxide of the late Pleistocene from Antarctic ice cores. Science 310, 1317–1321.
Still, C.J., Berry, J.A., Collatz, G.J., DeFries, R.S., 2003. Global distribution of C_3 and C_4 vegetation: carbon cycle implications. Global Biogeochemical Cycles 17.
Tans, P., 1997. A note on isotopic ratios and the global atmospheric methane budget. Global Biogeochemical Cycles 11, 77–81.
Valdes, P.J., Beerling, D.J., Johnson, C.E., 2005. The ice age methane budget. Geophysical Research Letters 32. doi:10.1029/2004GL021004.
Valentine, D.L., Chidthaisong, A., Rice, A., Reeburgh, W.S., Tyler, S.C., 2004. Carbon and hydrogen isotope fractionation by moderately thermophilic methanogens. Geochimica et Cosmochimica Acta 68, 1571–1590.
Waldron, S., Lansdown, J.M., Scott, E.M., Fallick, A.E., Hall, A.J., 1999. The global influence of the hydrogen isotope composition of water on that of bacteriogenic methane from shallow freshwater environments. Geochimica et Cosmochimica Acta 63, 2237–2245.
Walter, K., Edwards, M., Grosse, G., Zimov, S., Chapin III, , 2007. Thermokarst lakes as a source of atmospheric CH_4 during the last deglaciation. Science 318, 633.
Walter, K.M., Chanton, J.P., Chapin III, F.S., Schuur, E.A.G., Zimov, S.A., 2008. Methane production and bubble emissions from arctic lakes: isotopic implications for source pathways and ages. Journal of Geophysical Research 113.
Wang, Y., Cheng, H., Edwards, R.L., He, Y., Kong, X., An, Z., Wu, J., Kelly, M., Dykoski, C., Li, X., 2005. The Holocene Asian monsoon: links to solar changes and north Atlantic climate. Science 308, 854.
Wanner, H., Beer, J., Bütikofer, J., Crowley, T.J., Cubasch, U., Flückiger, J., Goosse, H., Grosjean, M., Joos, F., Kaplan, J.O., Küttel, M., Müller, S.A., Prentice, I.C., Solomina, O., Stocker, T.F., Tarasov, P., Wagner, M., Widmann, M., 2008. Mid- to Late Holocene climate change: an overview. Quaternary Science Reviews 27, 1791–1828.
Whiticar, M., Schaefer, H., 2007. Constraining past global tropospheric methane budgets with carbon and hydrogen isotope ratios in ice. Philosophical Transactions of the Royal Society 365, 1793–1828.
Whiticar, M.J., Faber, E., 1986. Methane oxidation in sediment and water column environments – isotope evidence. Organic Geochemistry 10, 759–768.